

Optical frequency comb with tunable free spectral range based on two Mach-Zehnder modulators cascaded with linearly chirped fiber Bragg grating and phase modulator*

GUAN Xiangshuai, MU Hongqian**, and WANG Muguang

Key Laboratory of All Optical Network and Advanced Telecommunication Network, Ministry of Education, Institute of Lightwave Technology, Beijing Jiaotong University, Beijing 100044, China

(Received 21 January 2022; Revised 5 April 2022)

©Tianjin University of Technology 2022

An approach for generating optical frequency comb (OFC) with tunable free spectral range (*FSR*) is proposed. Two Mach-Zehnder modulators (MZMs) driven by phase-shifted sinusoidal signals are cascaded to generate OFC with plentiful comb lines and the *FSR* controlled by the drive frequency. Subsequently, a linearly chirped fiber Bragg grating (LCFBG) and a phase modulator (PM) are used to increase the comb *FSR* by a particular integer multiple. Therefore, by simultaneously controlling the drive frequency of MZMs, the dispersion amount of the LCFBG and the drive signal of the PM, an OFC with desired *FSR* can be achieved.

Document code: A **Article ID:** 1673-1905(2022)07-0385-5

DOI <https://doi.org/10.1007/s11801-022-2011-z>

Optical frequency comb (OFC) has attracted much attention due to the ability to provide equally spaced and precise spectral lines for telecommunications and microwave photonics^[1-3], such as wavelength division multiplex^[4], optical frequency metrology^[5], and arbitrary waveform generation^[6]. Especially, an OFC that can simultaneously provide a large number of comb lines and any desired free spectral range (*FSR*) has become a hot topic. Mode-locked lasers and nonlinear effects in a highly nonlinear medium are commonly used methods to generate OFCs. Mode-locked lasers can generate OFC with ultra-large frequency span but fixed *FSR*^[7]. Using nonlinear effects in the highly nonlinear medium, the generated OFC suffers from flatness problems and lacks continuous tunability^[8]. In addition, the OFC generation approach based on a recirculating frequency shifting loop could provide a large number of comb lines with tunable *FSR*. Nevertheless, the generated comb lines lack long-term stability^[9].

Thanks to the excellent flexibility and stability, the OFC generation scheme based on external modulation of a continuous-wave (CW) laser has been widely investigated, such as using one dual-drive Mach-Zehnder modulator (MZM)^[10], two cascaded MZMs^[11], or one MZM cascaded with one phase modulator (PM)^[12]. Above listed combs, *FSRs* are all equal to the corresponding frequency of the sinusoidal drive signal and

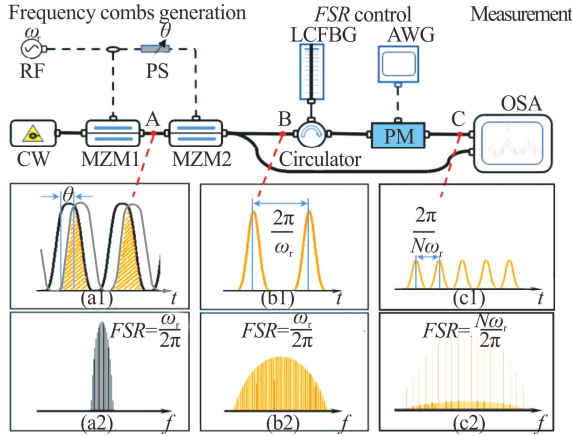
can be tuned by changing the drive frequency. However, it is difficult to realize large *FSR* because of the high cost of high-frequency sinusoidal signal source. Using two cascaded push-pull MZMs, CHONG et al^[13] achieved an OFC whose *FSR* is twice the frequency of sinusoidal drive signal. Based on coupled sinusoidal drive signal and a single MZM, XIE et al^[14] also realized an OFC whose *FSR* is twice the frequency of sinusoidal drive signal.

In order to practically achieve an OFC with a large number of comb lines and tunable *FSR*, we propose a novel OFC generation approach employing two MZMs, a linearly chirped fiber Bragg grating (LCFBG) and a PM. First, two MZMs are cascaded to output an OFC with a large number of equal-spaced comb lines. The comb *FSR* is tuned by adjusting the frequency of the sinusoidal drive signal. This means the maximum *FSR* is limited by the highest frequency of the sinusoidal signal source. In order to increase the comb *FSR* by a positive integer multiple, the temporal self-imaging (TSI) effect and the temporal phase compensation are introduced by controlling the chromatic dispersion amount of the LCFBG and the drive signal of the PM^[15,16]. Thus, the modified comb *FSR* at the output of the PM becomes multiple times as high as the frequency of the sinusoidal drive signal. In this way, we can realize an OFC with a large number of comb lines and desired *FSR* at a lower cost.

* This work has been supported partially by the National Natural Science Foundation of China (Nos.62101027 and 61775015), and the Fundamental Research Funds for the Central Universities (No.2019JBM010).

** E-mail: hongqianmu@bjtu.edu.cn

The schematic diagram of the proposed OFC with tunable FSR is depicted in Fig.1. A CW laser with optical field of $E_{in}(t)=E_0\exp(j\omega_0 t)$ is modulated by a sinusoidal signal with the angular frequency of ω_r , where E_0 and ω_0 are the amplitude and frequency of the optical carrier. The sinusoidal signal is first split by an electrical coupler and then drives MZM1 and MZM2 with a relative phase difference θ ($0<\theta<180^\circ$) introduced by a phase shifter (PS).



PS: phase shifter; CW: continuous-wave laser; MZM: Mach-Zehnder modulator; LCFBG: linearly chirped fiber Bragg grating; AWG: arbitrary waveform generator; PM: phase modulator; OSA: optical spectrum analyzer

Fig.1 Schematic diagram of the proposed OFC with tunable FSR: (a1) Process of pulse width reduction by tuning the phase shift θ ; (b1) Output pulse with reduced pulse width; (c1) Pulse train with multiplied repetition rate; (a2), (b2) and (c2) are the optical spectra corresponding to (a1), (b1) and (c1), respectively

The output optical field of MZM1 (at point A) is written as

$$E_A(t) = \frac{E_{in}(t)}{2} \left\{ \exp[j\pi \frac{V_1(t)}{V_\pi}] + \exp[j\pi \frac{V_2(t)}{V_\pi}] \right\}, \quad (1)$$

where V_π is the half-wave voltage, and $V_1(t)$ and $V_2(t)$ are the electrical drive signals applied to the upper and lower arms of MZM1, respectively. We set $V_1(t)=-V_2(t)=(V_{DC}+V_{RF}\sin\omega_r t)/2$, where V_{DC} and V_{RF} are the DC bias and the amplitude of the sinusoidal signal, respectively, and thus Eq.(1) is rewritten as

$$E_A(t) = \frac{E_{in}(t)}{2} \left\{ \exp[j\pi \frac{(V_{DC} + V_{RF} \sin \omega_r t)}{2V_\pi}] + \exp[-j\pi \frac{(V_{DC} + V_{RF} \sin \omega_r t)}{2V_\pi}] \right\} = \frac{E_{in}(t)}{2} [\exp(j\beta \sin \omega_r t) \exp(j\varphi) + \exp(-j\beta \sin \omega_r t) \exp(-j\varphi)], \quad (2)$$

where $\beta=\pi V_{RF}/2V_\pi$, $\varphi=\pi V_{DC}/2V_\pi$. When $V_{RF}=V_{DC}=V_\pi/2$, Eq.(2) is expressed by

$$E_A(t) = \frac{E_{in}(t)}{2} \exp(j\beta) [\exp(j\beta \sin \omega_r t) - j \exp(-j\beta \sin \omega_r t)]. \quad (3)$$

Using Bessel functions of the first kind, Eq.(3) is expanded as

$$E_A(t) = \frac{E_0 \exp(j\beta)}{2} \{ [J_0(\beta) - jJ_1(\beta)] \exp(j\omega_0 t) + \sum_{n=1}^{+\infty} (-1)^n [(J_n(\beta) - jJ_n(\beta))] \exp[j(\omega_0 \pm n\omega_r)t] \}. \quad (4)$$

The first term in Eq.(4) represents the center frequency of the OFC, while the second term creates the rest of the comb lines. The frequency spacing between the comb lines is governed by the frequency of the sinusoidal drive signal ω_r . In order to increase the number of comb lines, the optical pulse width ought to be decreased by cascading MZM2. Under the condition of $V_{RF}=V_{DC}=V_\pi/2$, the output optical field of MZM2 (at point B) is given by

$$E_B(t) = \frac{E_A(t)}{2} \{ \exp[j\beta \sin(\omega_r t + \theta)] \exp(j\varphi) + \exp[-j\beta \sin(\omega_r t + \theta)] \exp(-j\varphi) \}. \quad (5)$$

Using Bessel functions of the first kind, Eq.(5) is expanded as

$$E_B(t) = \frac{E_0}{4} \exp(j2\beta) \left\{ \sum_{n=-\infty}^{+\infty} [J_n(\beta) - jJ_n(\beta)] \times \exp[j(\omega_0 + n\omega_r)t] \right\} \times \left\{ \sum_{m=-\infty}^{+\infty} [J_m(\beta) - jJ_m(\beta)] \exp[jm(\omega_r t + \theta)] \right\}. \quad (6)$$

By tuning the phase shift θ , the pulse width at point B can be reduced, and the number of comb lines is increased accordingly. Nevertheless, the comb FSR remains the same as the frequency of the sinusoidal drive signal, as shown in Fig.1(a2) and Fig.1(b2).

Subsequently, the process of comb FSR multiplication is enabled by the combination of LCFBG and PM, as shown in Fig.2. The LCFBG is used to introduce the TSI effect, and the PM is used to compensate for the residual phase variations. According to the theory of the TSI effect^[17], when the dispersion amount D (ps/nm) of the LCFBG satisfies

$$|D| = \frac{Mct_r^2}{N\lambda_0^2}, \quad (7)$$

the reflected pulse repetition rate of the LCFBG becomes N times of the input pulse repetition rate (Fig.2(a2)), where N and M are two mutually prime integers, c is the light speed in a vacuum, t_r is the input pulse period of LCFBG and λ_0 is the central wavelength of the comb spectra. The maximum N ought to be limited to avoid the overlap of the adjacent pulses. It depends on the ratio of the repetition rate of input pulse to the pulse width. As the signal representations in the time domain and frequency domain have unrelated repetition periods, the reflected comb FSR remains the same as the input comb FSR to LCFBG, as shown in Fig.2(b1) and Fig.2(b2). As the temporal phase profile of the LCFBG-reflected pulse

train has a parabolic envelope^[18,19], a PM is inserted to compensate the residual phase variations of the pulse train so that every optical pulse has the same phase, as shown in Fig.2(a3). The phase of the n -th optical pulse is set to be

$$\varphi_n = \frac{s}{m} \pi n^2 \quad (n = 0, \pm 1, \pm 2, \dots), \quad (8)$$

where s and m are coprime integers, and $m=N$ is the FSR multiplication factor. It is worth noting that φ_n is periodic with period $2m$ when the product of s and m is odd, or with period m when the product of s and m is even. In other words, we need to perform a periodic temporal phase modulation that contains $2m$ or m discrete phase levels in each period. After the temporal phase compensation, the comb FSR becomes N times of the original one, as shown in Fig.2(b3). Based on the above theory, as both the frequency ω_s of the sinusoidal drive signal and the FSR multiplication factor N are tunable, the proposed OFC generation system is capable of realizing an OFC with a large number of comb lines and tunable FSR . The maximum FSR depends on the product of the highest frequency of the sinusoidal signal source and the ultimate FSR multiplication factor.

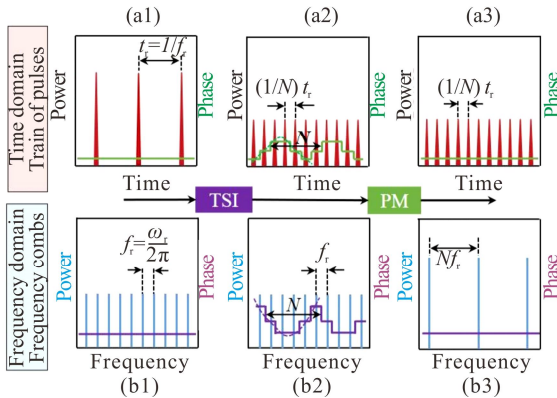


Fig.2 Process of the comb FSR multiplication: (a1)–(a3) Signal representations in the time domain; (b1)–(b3) Signal representations in the frequency domain

Next, we present several simulation results of the proposed system based on the OptiSystem platform. As shown in Fig.3, a lightwave with the wavelength of 1 550 nm and the output power of 20 dBm is emitted by a CW laser and then sent to two cascaded MZMs. A sinusoidal signal is split into two paths to drive the two MZMs with a relative phase shift θ controlled by a PS. Fig.4(a) illustrates the variations of the pulse width and pulse power with θ , in which points P, Q, and R are selected to show the waveforms in detail (Fig.4(b)). It can be seen that the pulse width decreases when θ increases. This is beneficial to realize the larger FSR multiplication factor. However, when the pulse width is reduced, the pulse power drops as well. When $\theta=120^\circ$, there exists a maximum difference between the pulse power and pulse

width (see points S and R). Jointly considering the pulse power and the pulse width, we set $\theta=120^\circ$.

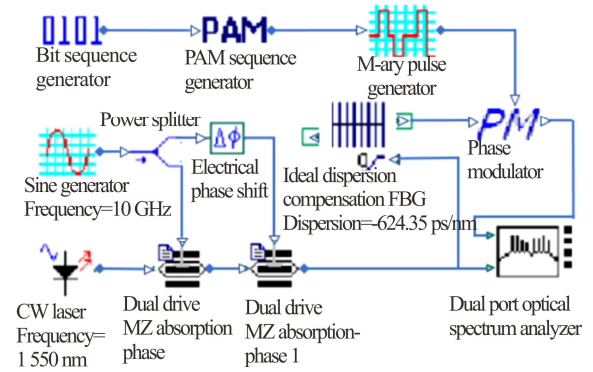


Fig.3 Simulation setup of the proposed OFC with tunable FSR

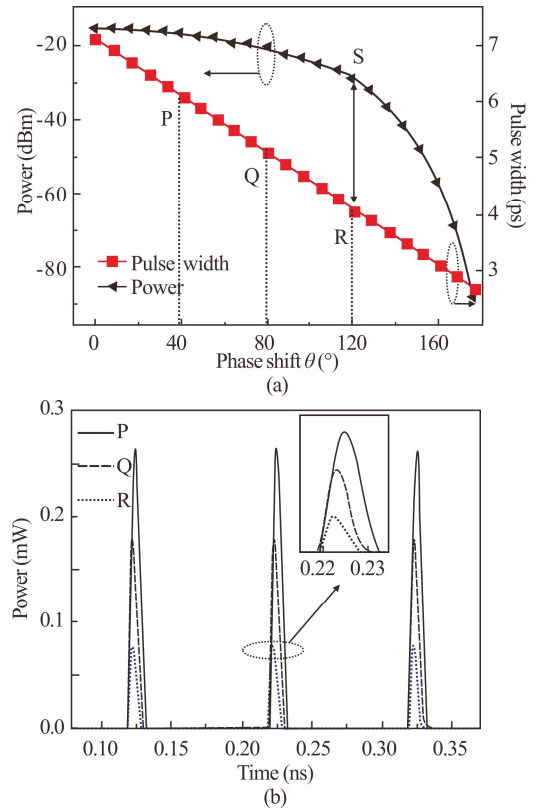


Fig.4 (a) Variations of the pulse width and pulse power with phase shift θ ; (b) Waveforms of points P, Q, and R in detail of (a)

The drive frequency of the sinusoidal signal source is set to be 10 GHz. Thus, the output comb FSR of two cascaded MZMs is 10 GHz. Subsequently, an LCFBG and a PM are connected to multiply this comb FSR . The dispersion value of the LCFBG is set at -624.35 ps/nm for an FSR multiplication factor of 2 ($M=1$, $N=2$ in Eq.(7)), and the PM is driven by an electrical periodic pulse sequence $\{0, \pi/2; 0, \pi/2, \dots\}$ ($s=1$, $m=2$ in Eq.(8)) to compensate residual phase variations of each optical

pulse. As a result, an OFC with 20 GHz *FSR* is obtained, as shown in Fig.5(a). Likewise, when the dispersion value of the LCFBG is set at -124.87 ps/nm for an *FSR* multiplication factor of 10 ($M=1, N=10$), and the PM is driven by an electrical periodic pulse sequence $\{0, \pi/10, 2\pi/5, 9\pi/10, 8\pi/5, \pi/2, 8\pi/5, 9\pi/10, 2\pi/5, \pi/10; 0, \pi/10, 2\pi/5, 9\pi/10, 8\pi/5, \pi/2, 8\pi/5, 9\pi/10, 2\pi/5, \pi/10\dots\}$ ($s=1, m=10$), an OFC with 100 GHz *FSR* is obtained as shown in Fig.5(b). For the above two cases, the resulting power of each spectral line is around 3 dB or 10 dB higher than that of the OFC at the output of two cascaded MZMs, indicating the high energy efficiency of this method.

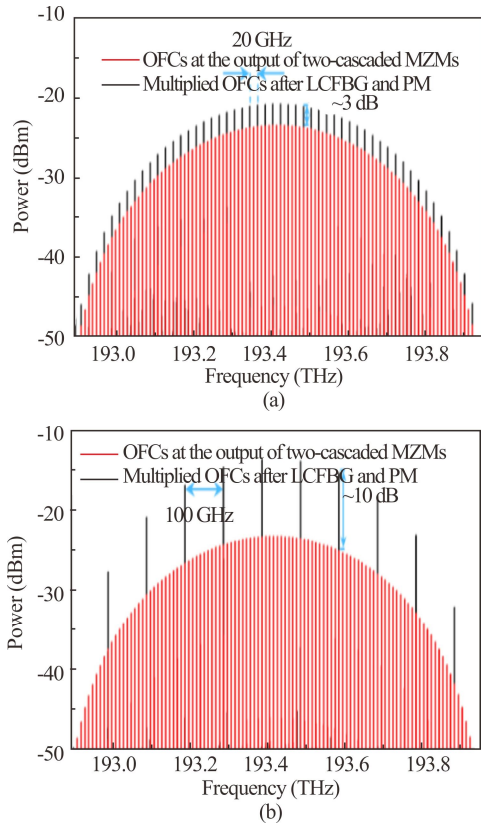


Fig.5 Measured OFCs at the output of two-cascaded MZMs and multiplied OFCs after LCFBG and PM with (a) *FSR* of 20 GHz and (b) *FSR* of 100 GHz

Finally, to verify the flexibility of the proposed approach, we vary both the drive frequency of the sinusoidal signal source and the *FSR* multiplication factor to generate OFCs with different *FSR* values. As shown in Fig.6(a), an OFC with 30 GHz *FSR* is realized by setting the sinusoidal drive frequency at 5 GHz and the *FSR* multiplication factor at 6, where the dispersion value of the LCFBG is -832.47 ps/nm ($M=1, N=6$) and the PM is driven by an electrical periodic pulse sequence $\{0, \pi/6, 2\pi/3, 3\pi/2, 2\pi/3, \pi/6; 0, \pi/6, 2\pi/3, 3\pi/2, 2\pi/3, \pi/6\dots\}$ ($s=1, m=6$). The resulting power of each spectral line is around 8 dB higher than that of the OFC at the output of two cascaded MZMs. In addition, as shown in Fig.6(b), an OFC with 64 GHz *FSR* is acquired by setting the si-

nusoidal drive frequency at 8 GHz and the *FSR* multiplication factor at 8, where the dispersion value of the LCFBG is -243.89 ps/nm ($M=1, N=8$) and the PM is driven by an electrical periodic pulse sequence $\{0, \pi/8, \pi/2, 9\pi/8, 0, 9\pi/8, \pi/2, \pi/8; 0, \pi/8, \pi/2, 9\pi/8, 0, 9\pi/8, \pi/2, \pi/8\dots\}$ ($s=1, m=8$). The resulting power of each spectral line is around 9 dB higher than that of the OFC at the output of two cascaded MZMs.

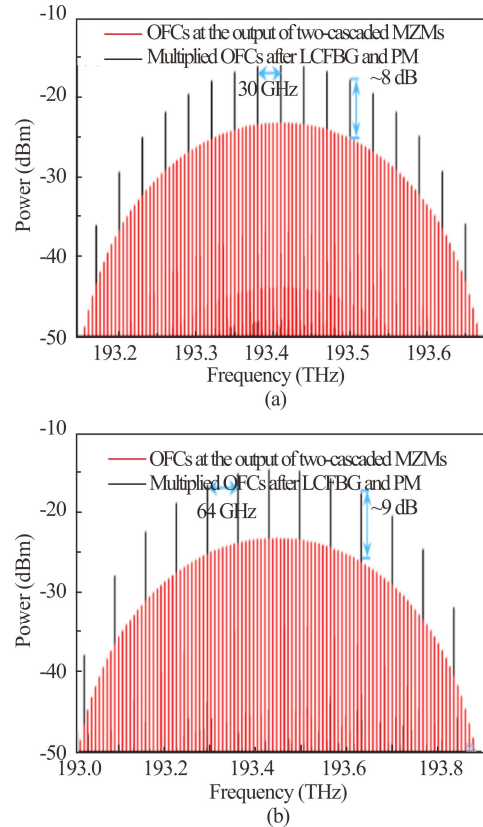


Fig.6 Measured OFCs at the output of two-cascaded MZMs and multiplied OFCs after LCFBG and PM with (a) *FSR* of 30 GHz and (b) *FSR* of 64 GHz

In conclusion, using two MZMs cascaded with an LCFBG and a PM, an approach for OFC generation with plentiful comb lines and tunable *FSR* has been proposed and demonstrated. In order to achieve an OFC with plentiful comb lines, two MZMs are driven by phase-shifted sinusoidal signals. Subsequently, LCFBG and PM are utilized to introduce the TSI effect and temporal phase compensation for the *FSR* multiplication. Since the frequency of the sinusoidal drive signal and the *FSR* multiplication factor are both tunable, an optical comb with the desired *FSR* can be achieved. The desired comb *FSR* can be tuned flexibly between 0 and the product of the highest frequency of the sinusoidal signal source and the maximum *FSR* multiplication factor. In the simulation, the highest frequency of the sinusoidal source is 10 GHz, and the maximum *FSR* multiplication factor is 10. Thus, the desired *FSR* of OFC could be tuned between 0 and 100 GHz. We have obtained OFCs whose *FSR* is 2, 6, 8,

and 10 times as high as the frequency of the sinusoidal drive signal. The simulation results agree well with the theoretical analysis. The proposed OFC generation approach may contribute to the development of cost-effective OFC with a large number of comb lines and tunable *FSR*.

Statements and Declarations

The authors declare that there are no conflicts of interest related to this article.

References

- [1] CAMPANY J, MORA J, GASULLA I, et al. Microwave photonic signal processing[J]. *Journal of lightwave technology*, 2013, 31(4): 571-586.
- [2] DIDDAMS S A. The evolving optical frequency comb[J]. *Journal of the optical society of America B*, 2010, 27(11): B51-B62.
- [3] PFEIFLE J, BRASCH V, LAUERMAN M, et al. Coherent terabit communications with microresonator Kerr frequency combs[J]. *Nature photonics*, 2014, 8(5): 375-380.
- [4] CHUN B J, HYUN S, KIM S, et al. Frequency-comb-referenced multi-channel fiber laser for DWDM communication[J]. *Optics express*, 2013, 21(24): 29179-29185.
- [5] GAGLIARDI G, SALZA M, AVINO S, et al. Probing the ultimate limit of fiber-optic strain sensing[J]. *Science*, 2010, 330(6007): 1081-1084.
- [6] ZHOU X, ZHENG X P, WEN H, et al. All optical arbitrary waveform generation by optical frequency comb based on cascading intensity modulation[J]. *Optics communications*, 2011, 284(15): 3706-3710.
- [7] DAVILA-RODRIGUEZ J, BAGNELL K, DELFYETT P J. Frequency stability of a 10 GHz optical frequency comb from a semiconductor-based mode-locked laser with an intracavity 10,000 finesse etalon[J]. *Optics letters*, 2013, 38(18): 3665-3668.
- [8] MELO S A S, DO NASCIMENTO A R, CERQUEIRA S A, et al. Frequency comb expansion based on optical feedback, highly nonlinear and erbium-doped fibers[J]. *Optics communications*, 2014, 312: 287-291.
- [9] JIANG W, ZHAO S H, LI X J, et al. Optical frequency comb generation based on three parallel Mach-Zehnder modulators with recirculating frequency shifting loop[J]. *Optical review*, 2017, 24(4): 533-539.
- [10] SAKAMOTO T, KAWANISHI T, IZUTSU M. Asymptotic formalism for ultraflat optical frequency comb generation using a Mach-Zehnder modulator[J]. *Optics letters*, 2007, 32(11): 1515-1517.
- [11] HEALY T, GARCIA G F C, ELLIS A D, et al. Multi-wavelength source using low drive-voltage amplitude modulators for optical communications[J]. *Optics express*, 2007, 15(6): 2981-2986.
- [12] ULLAH S, ULLAH R, ZHANG Q, et al. Ultra-wide and flattened optical frequency comb generation based on cascaded phase modulator and LiNbO₃-MZM offering terahertz bandwidth[J]. *IEEE access*, 2020, 8: 76692-76699.
- [13] CHONG Y H, YANG C, LI X H, et al. Generation of optical frequency comb with double spectral spacing based on two cascaded push-pull Mach-Zehnder modulators[C]//*International Photonics and OptoElectronics Meetings 2014*, June 18-21, 2014, Wuhan, China. Washington: Optical Society of America, 2014: FTh4E.4.
- [14] XIE H L, JIA K X, CHEN J W, et al. Tunable optical frequency comb based on coupled radio frequency signal and single Mach-Zehnder modulator[J]. *Chinese journal of lasers*, 2020, 47(7): 0706002.
- [15] AZANA J, MURIEL M A. Temporal self-imaging effects: theory and application for multiplying pulse repetition rates[J]. *IEEE journal of selected topics in quantum electronics*, 2001, 7(4): 728-744.
- [16] CARAQUITENA J, BELTRAN M, LLORENTE R, et al. Spectral self-imaging effect by time-domain multi-level phase modulation of a periodic pulse train[J]. *Optics letters*, 2011, 36(6): 858-860.
- [17] AZANA J, GUPTA S. Complete family of periodic Talbot filters for pulse repetition rate multiplication[J]. *Optics express*, 2006, 14(10): 4270-4279.
- [18] FERNANDEZ-POUSA C R. On the structure of quadratic Gauss sums in the Talbot effect[J]. *Journal of the optical society of America A*, 2017, 34(5): 732-742.
- [19] ROMERO C L, MARAM R, GUILLET D C H, et al. Arbitrary energy-preserving control of optical pulse trains and frequency combs through generalized Talbot effects[J]. *Laser & photonics reviews*, 2019, 13(12): 1900176.